Simulations of planar non-thermal plasma assisted ignition at atmospheric pressure

SAND2016-6931C

36th Combustion Symposium, Seoul

08/05/16

Tiernan Casey[a]

Jie Han[b], Memdouh Belhi[b], Paul Arias[c], Fabrizio Bisetti[b], Hong Im[b], Jyh-Yuan Chen[a]

[a]University of California, Berkeley

[b]King Abdullah University of Science and Technology

[c]University of Michigan

NSF CBET-1510709

KAUST

KAUST AEA

Berkeley
UNIVERSITY OF CALIFORNIA

Electric field effects: background

- Flame zones are essentially weakly ionized plasmas, generate weak self-electric fields due to local charge separation
- As such, externally applied electric fields have the ability to augment flames “non-intrusively”
- Applied electric fields have been observed to affect reacting flows by:
  - enhancing burning velocities
  - extending flammability limits (lean)
  - supporting ignition

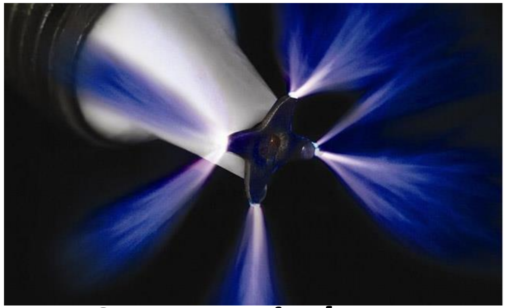

Corona Discharge Ignition System

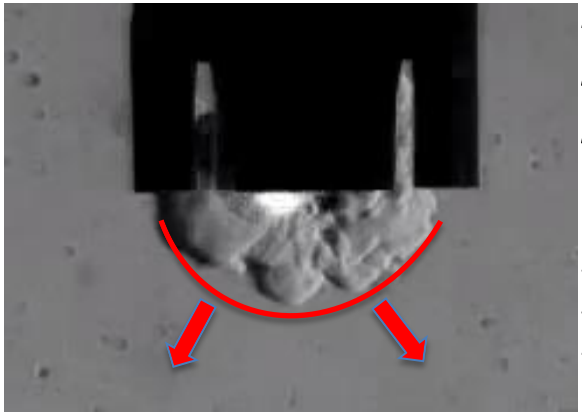

Pulsed plasma breakdown ignition device

[1] D. I. Pineda, et al., "Nanosecond Pulsed Discharge in a Lean Methane-Air Mixture," in Laser Ignition Conference, OSA Technical Digest (online) (Optical Society of America, 2015), paper T5A.2.

Berkeley
UNIVERSITY OF CALIFORNIA

Conceptual motivation

- thermal effects: energy transfer from accelerated electrons to neutral molecules results in bulk fluid heating

- chemical effects: energetic electron collisions with abundant neutral molecules (e.g. N_2, O_2 in air) generate excited states, ions, with increased reactivity, cause decomposition

- electro-hydrodynamic force: acceleration of ions and electrons by electric fields, resulting in increased momentum of the bulk fluid

Electron fluid

- Strong electric fields acting on charged species can cause bulk fluid approximations to break down
- Must derive individual fluid equations for possible non-equilibrium components (electron fluid), e.g. using moments of the Boltzmann kinetic equation

$$\frac{\partial m_e n_e}{\partial t} + \nabla \cdot (m_e n_e u_e) = S_e$$

electron fluid mass conservation

$$\frac{\partial m_e n_e u_e}{\partial t} + \nabla \cdot (m_e n_e u_e u_e) = -\nabla p_e - e n_e E - m_e n_e \nu_{en} (u_e - u_n)$$

electron fluid momentum conservation

species body force

collisional drag force (Lorentz gas model)

Zero-inertia approximation for electron fluid momentum

$$n_e u_e = -\frac{e}{m_e \nu_{en}} n_e E - \frac{1}{m_e \nu_{en}} \nabla (n_e k_B T_e)$$

Berkeley
UNIVERSITY OF CALIFORNIA

Electron fluid

This defines an electron fluid transport coefficient:

- electron mobility

$$\mu_e = \frac{e}{m_e \nu_{en}}$$

- electron momentum eq. is now algebraic

$$n_e u_e = -\mu_e n_e E - D_e \nabla n_e$$

"drift" *"diffusion"*

- electron flux is closed with specification of the collision frequency, which can be estimated from kinetic theory and knowledge of the energy/speed distribution function

Berkeley
UNIVERSITY OF CALIFORNIA

Governing equations

1 Electron fluid

$$\frac{\partial n_e}{\partial t} + \nabla \cdot (n_e \mathbf{u}_e) = S_e \qquad \mathbf{u}_e = -\frac{e}{m_e \nu_e}\mathbf{E} - \frac{1}{n_e m_e \nu_e}\nabla (n_e k_B T_e)$$

2 Bulk fluid

$$\frac{\partial \rho Y_i}{\partial t} + \nabla \cdot (\rho Y_i [\mathbf{u} + \mathbf{V_i}]) = m_i S_i$$

Electron Drag

$$\frac{\partial \rho \mathbf{u}}{\partial t} + \nabla \cdot (\rho \mathbf{u}\mathbf{u}) = -\nabla p + \nabla \cdot \tau + \rho_q \mathbf{E} - \sum_{s \neq e} n_s m_{s,e} \nu_{s,e} (\mathbf{u_s} - \mathbf{u_e})$$

$$\frac{\partial \rho e_T}{\partial t} + \nabla \cdot (\rho \mathbf{u} e_T) = -\nabla \cdot \mathbf{Q} + \nabla \cdot (\underline{\sigma} \cdot \mathbf{u}) - \sum_{s \neq e} 3 n_e \frac{m_s}{m_e} \nu_{s,e} k_B (T_s - T_e) + (\epsilon_{cons} S_{e,cons} - \epsilon_{prod} S_{e,prod})$$

Electron elastic energy transfer model

Electron inelastic energy exchanges

Gauss' Law

$$\epsilon \nabla \cdot \mathbf{E} = \sum_{s \neq e} \left(\frac{\rho q_s Y_s}{m_s} \right) - e n_e$$

s: species (electron or bulk component)

e: electron species

i: bulk fluid components

Berkeley

UNIVERSITY OF CALIFORNIA

Example: Laminar premixed methane-air flame

- Stoichiometric mixture, 300K fresh gas at 1atm, 0V boundaries on 3cm domain, left end inlet, right end open

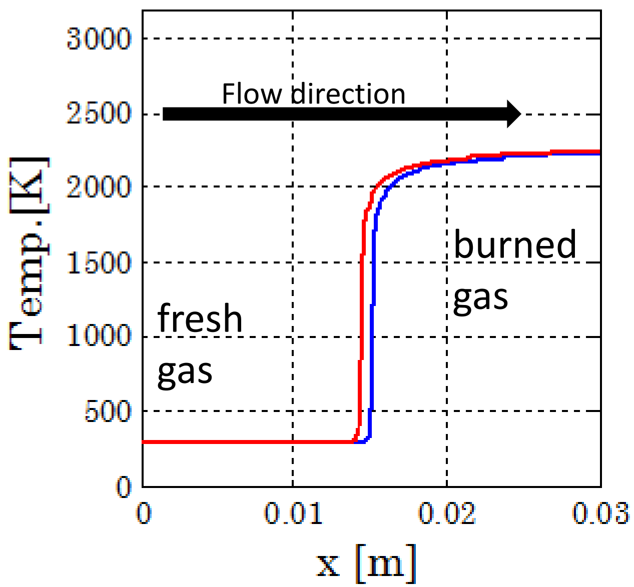

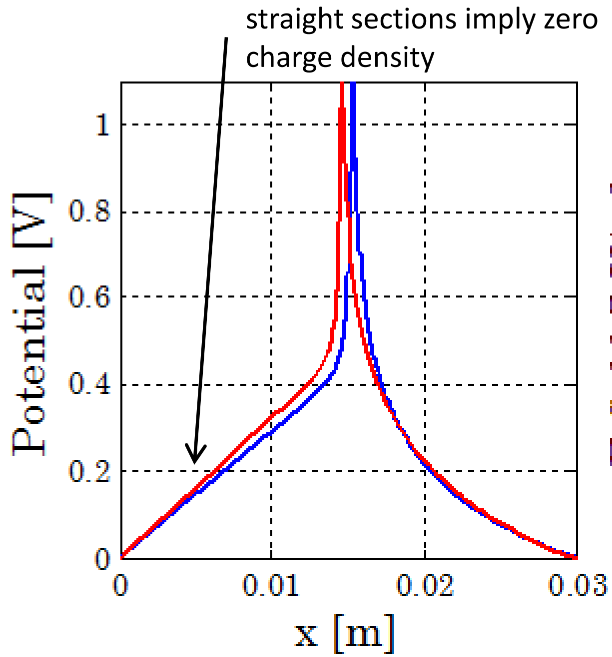

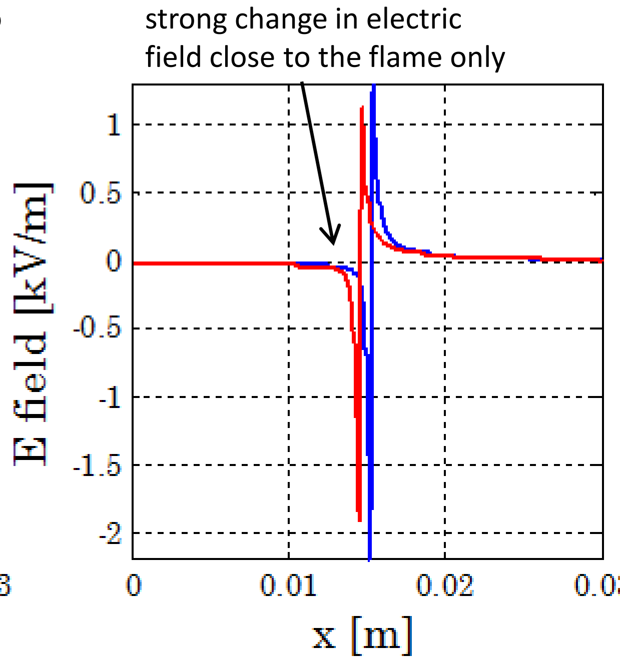

Blue curves are **transient** results (S3D)
Red curves are **steady-state** results using an equilibrium solver (PREMIX)

KAUST

Berkeley
UNIVERSITY OF CALIFORNIA

Laminar premixed flames

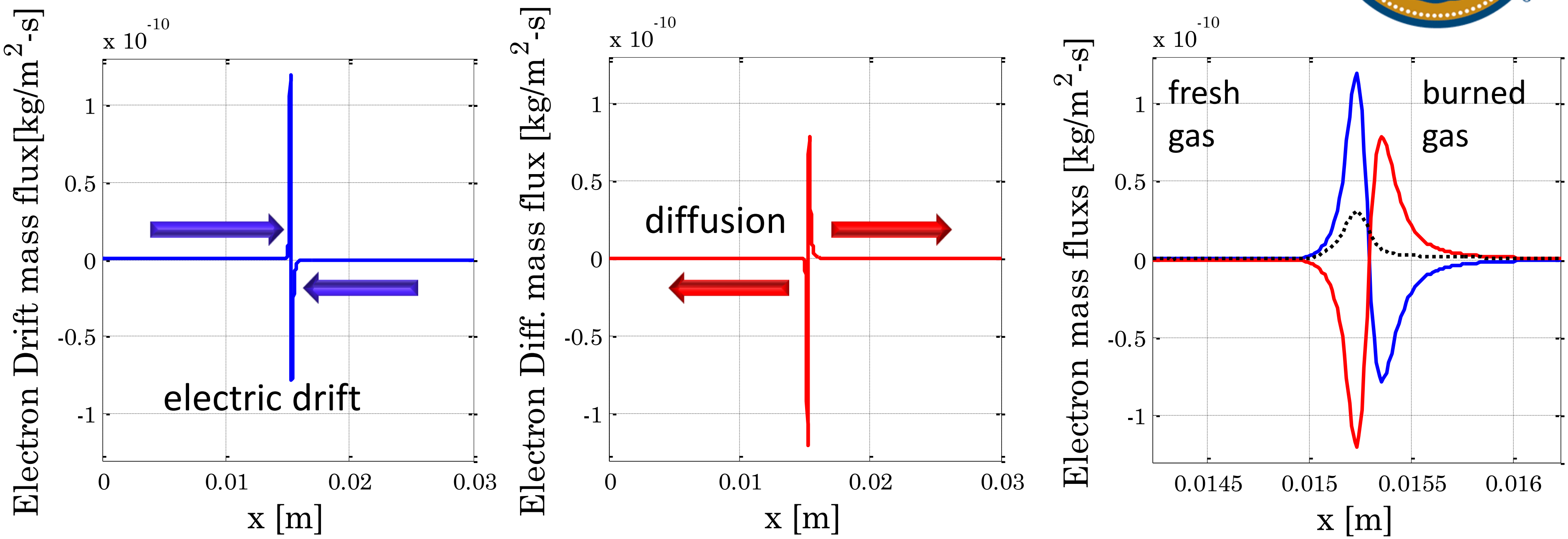

- Self-field dynamic equilibrium: mass fluxes are in balance, a pool of electrons sits at the flame

Berkeley
UNIVERSITY OF CALIFORNIA

Electron properties

- Electron Boltzmann eq. solver: BOLSIG+

http://www.bolsig.laplace.univ-tlse.fr/

- Two term approximation for phase space electron density
- Problem is fully posed by specification of the neutral species densities (chemistry), gas temperature (energy loss), and electric field

Electron mobility (laminar flame):

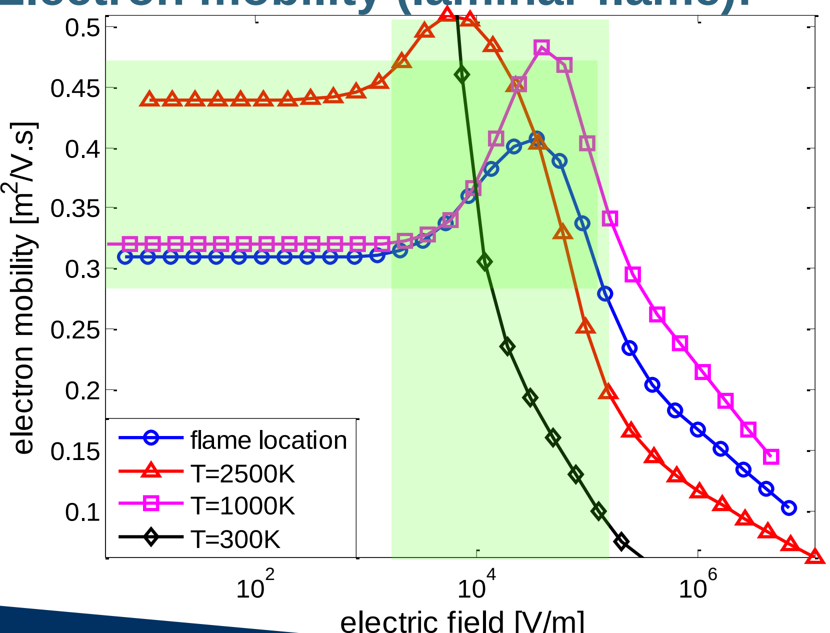

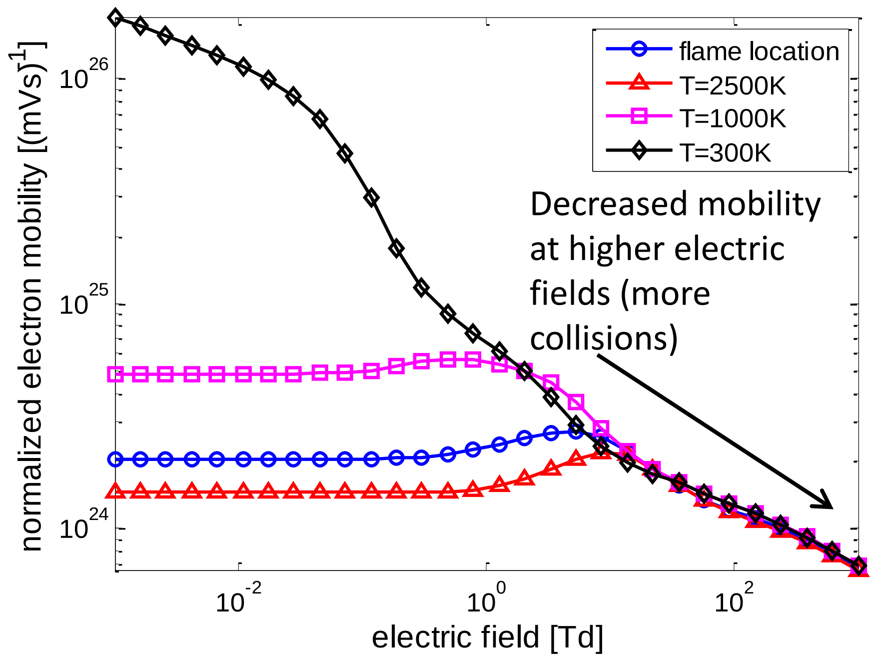

Berkeley
UNIVERSITY OF CALIFORNIA

Numerics

- Reacting Navier-Stokes equations: fully compressible transient reacting flow simulations in 1D, conservative finite difference discretization (S3D, MPI using 32 threads)
- 4^{th} order low-storage Runge-Kutta explicit time integration, time step at typically 1ns (thermal plasma), 6^{th} order centered spatial differencing scheme, 8µm resolution
- 45 species methane-air chemical model with two-temperature parameterization, non-thermal electron impact reactions using CHEMKIN. Factor of 2 speed up by pre-computing rate constants.
- Poisson equation for Gauss' law solved using geometric multigrid iterative methods
- transport properties and electron energies pre-computed using the BOLSIG+ solver, interpolated at runtime

Plasma assisted ignition

- Standard ignition devices (spark) use discharge arcs as energy sources for ignition. But increasing spark energy can result in decreased device life due to ablation
- Instead propose to use applied electric fields to support weak ignition kernels
- Emulate pulsed plasma assisted ignition using a single square wave pulse of 10kV magnitude and ~ns duration applied to a developing ignition kernel
- Interested in atmospheric pressure for device and experimental conditions

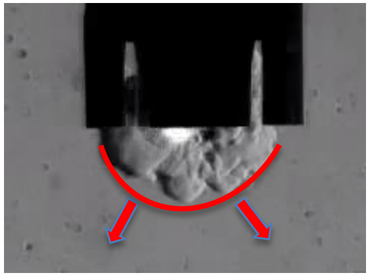

nanosecond pulsed plasma ignition device

Berkeley
UNIVERSITY OF CALIFORNIA

Planar ignition: CH_4-Air (unsupported)

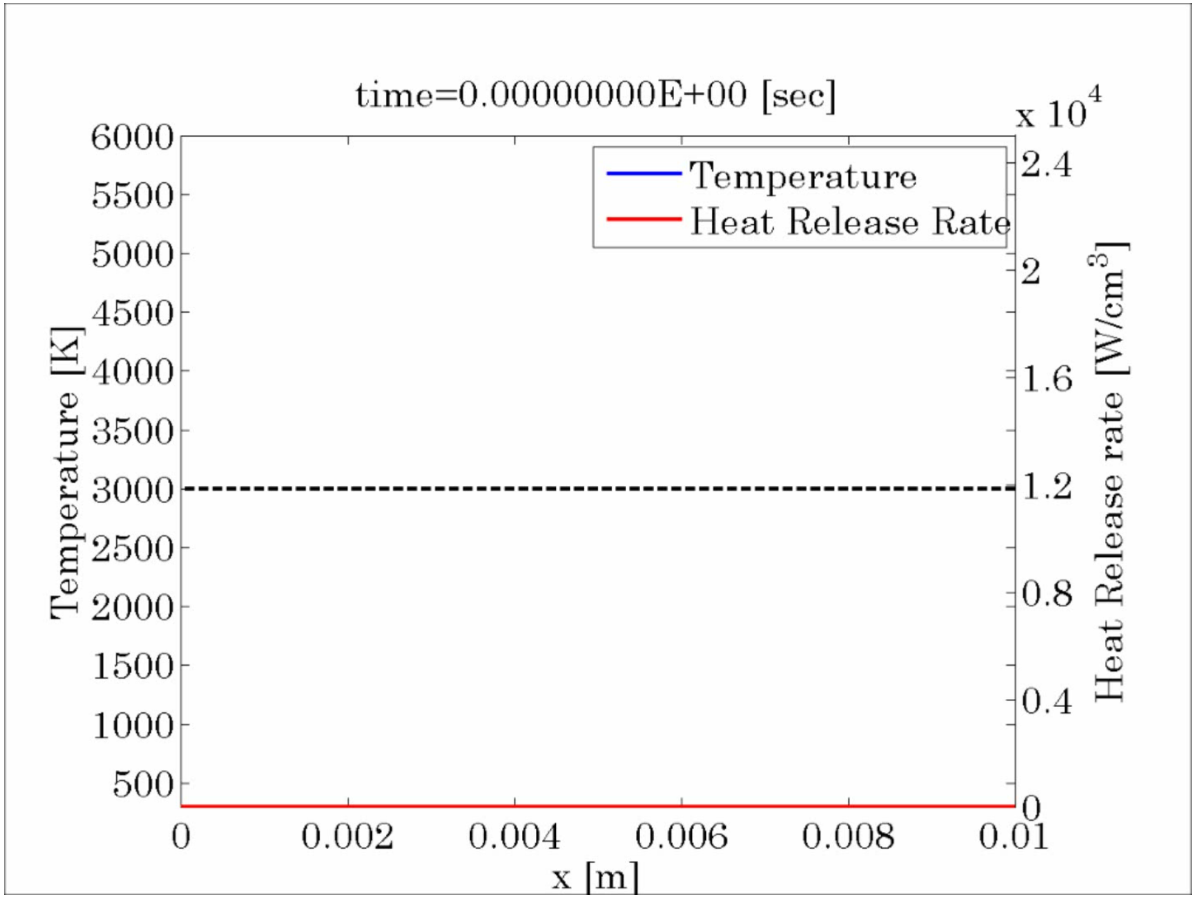

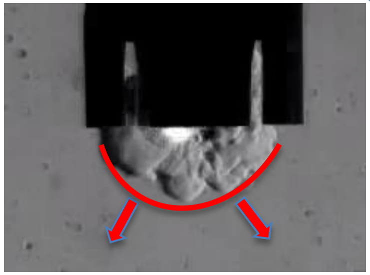

- 1cm domain
- fluid ignited by Gaussian shaped ignition kernel active for 80µs, 85mJ total energy
- boundaries are non-obstructive to fluid (mesh electrodes)
- ends grounded

Planar ignition: CH_4-Air

- Flame fronts propagate outwards rapidly
- Begin to decelerate as they depart from the hottest regions of burned gas and back-support diminishes
- What happens when a strong electric field is applied? (ns pulse)

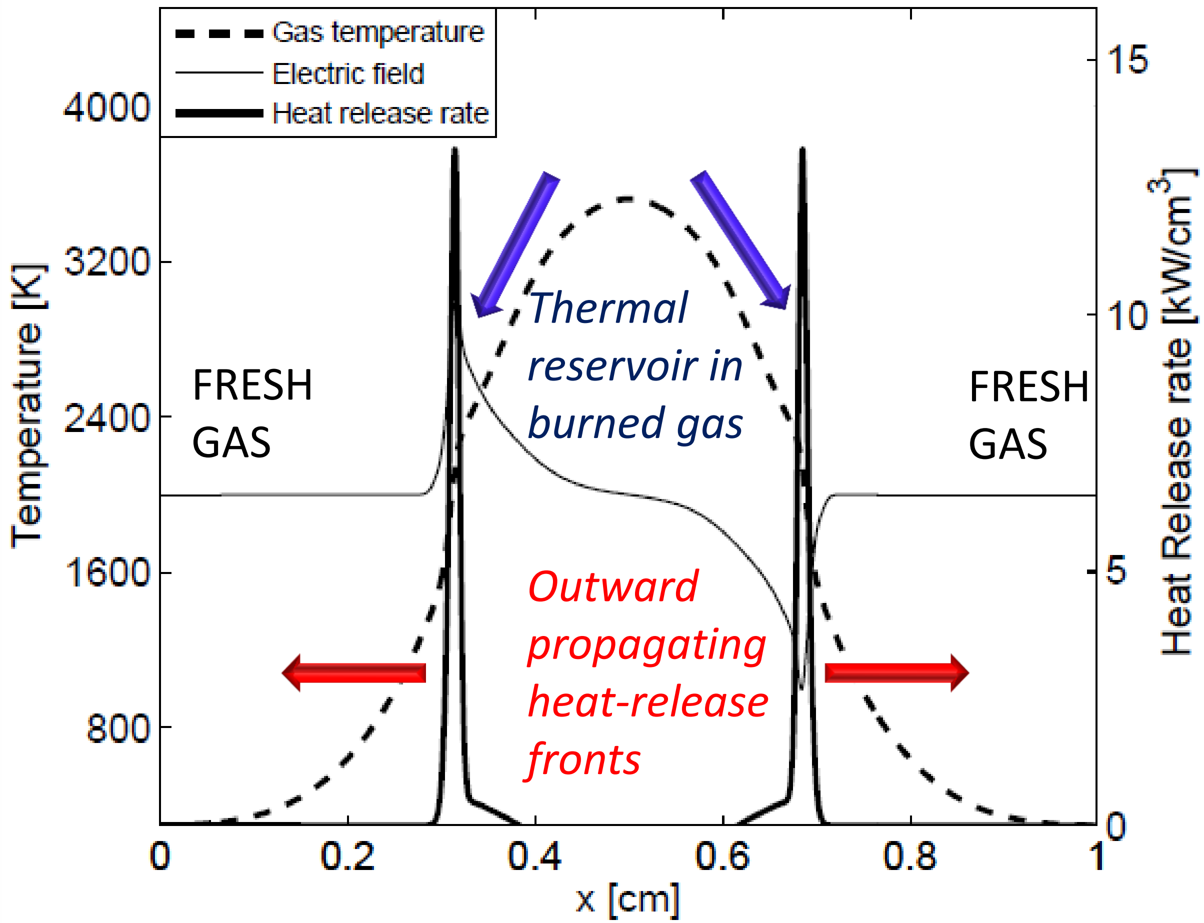

Planar ignition support – DC pulse

- DC pulses, 20ns-35ns duration, 10kV (-5kV left, +5kV right)
- 300K mixture, 1atm, ϕ=0.5
- Electrons rapidly become non-thermal due to Joule heating, activate impact chemistry
- Simulation $\Delta t = 10^{-13}$s to resolve electron impact kinetic rates during pulse, relax dynamically to $\Delta t = 10^{-9}$s post pulse

total (domain integrated) electron density

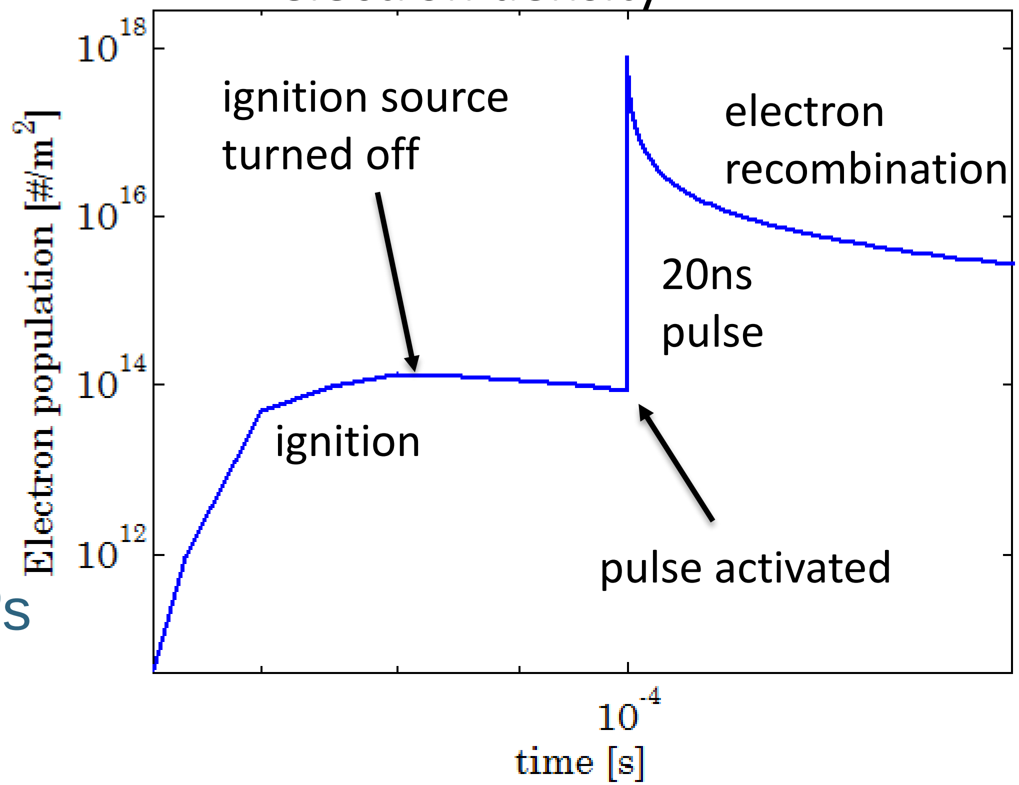

Berkeley
UNIVERSITY OF CALIFORNIA

Instantaneous ignition profiles during pulse

instantaneous potential field

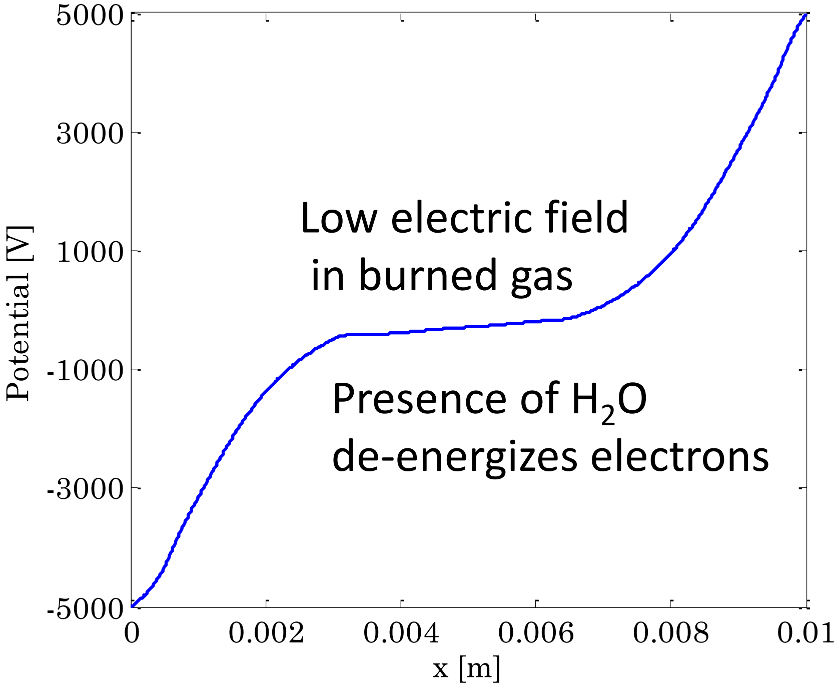

instantaneous electron temperature

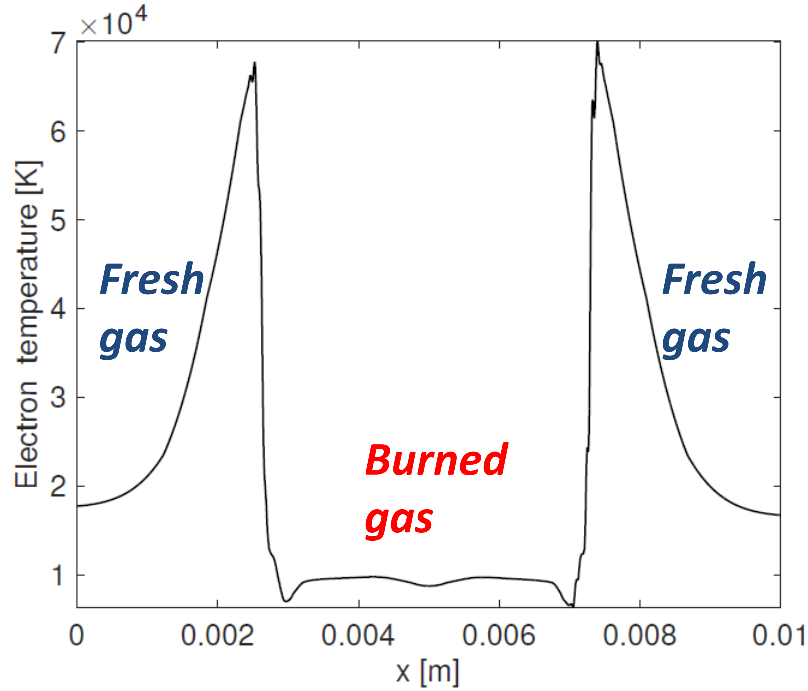

- electron temperature ~20,000-70,000 K in fresh gas
- electron temperature is conjugate to electric field strength

Berkeley
UNIVERSITY OF CALIFORNIA

Dynamics of charge fronts

- On pulse activation, charge originating in the flame zones is ejected into the fresh gases
- As the charge front advances, ionization processes increase the charge density
- Post pulse, the charge fronts collapse due to recombination

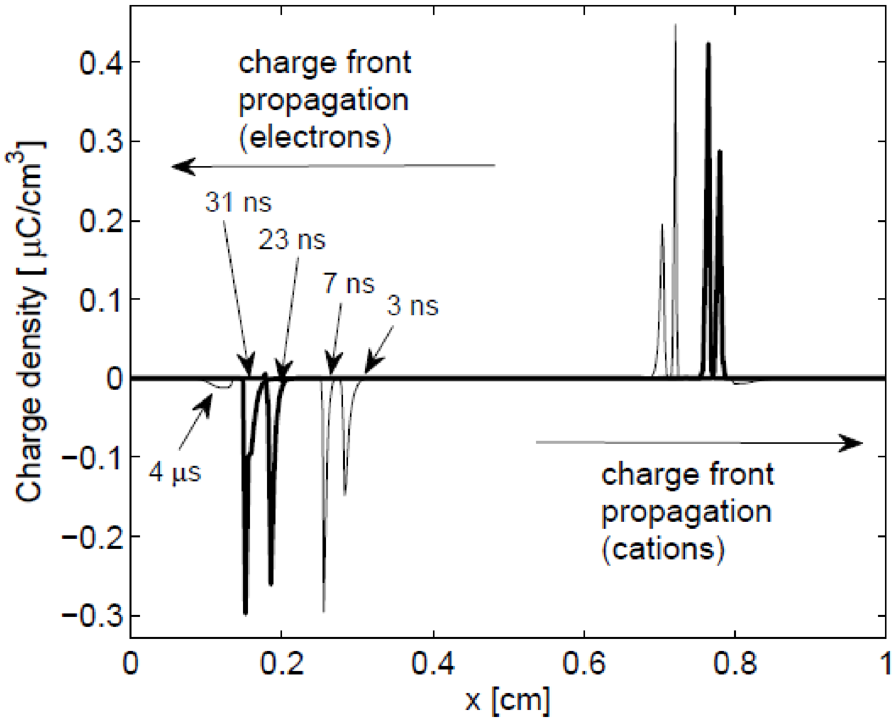

Charge front propagation for 35ns pulse. Electrons are swept to the left, cations are swept to the right

Berkeley
UNIVERSITY OF CALIFORNIA

Electric field compression

- Charge fronts are very pronounced, changes in electric field are restricted to their vicinity
- this results in a “floating electrode” effect as the potential transitions from linear to a constant value
- the advancing charge fronts steepen the slope of the potential, increasing the electric field strength

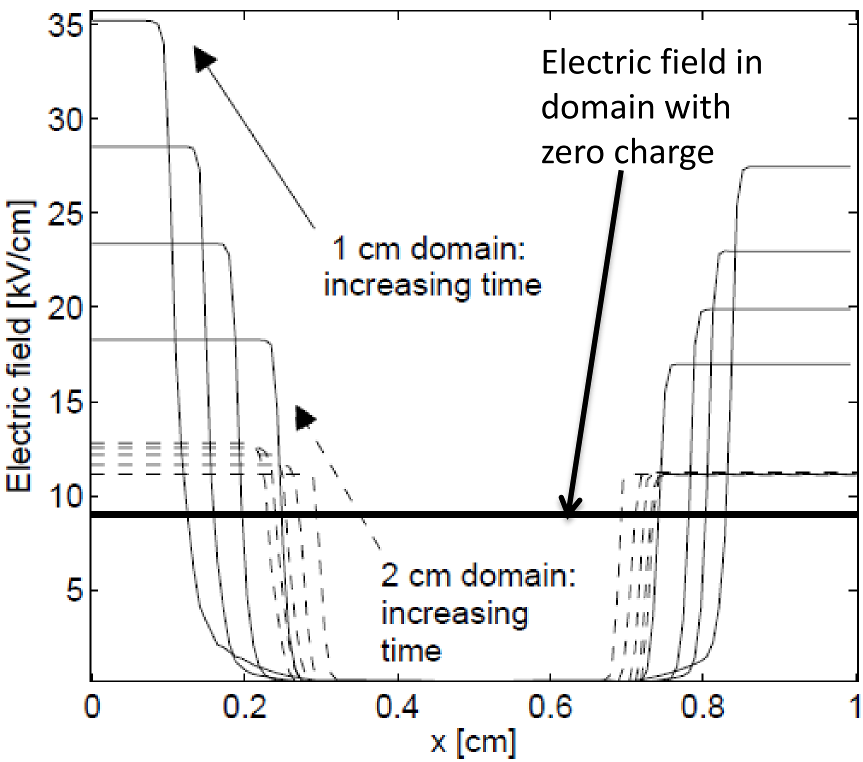

Increase in electric field strength between end electrodes and charge fronts

Production and consumption

Electrons streaming into the fresh gas result in CH_4 decomposition and further electron production

1: electron production is high, a large packet of thermal electrons in the reaction zone. CH_4 consumption increases

2: electrons are ejected from reaction zone cause impact ionization (producing more electrons), CH_4 impact decomposition occurs

3-5: ionization processes not increasing, CH_4 impact decomposition and de-excitation of electronically excited N_2 (also increasing electron temperature)

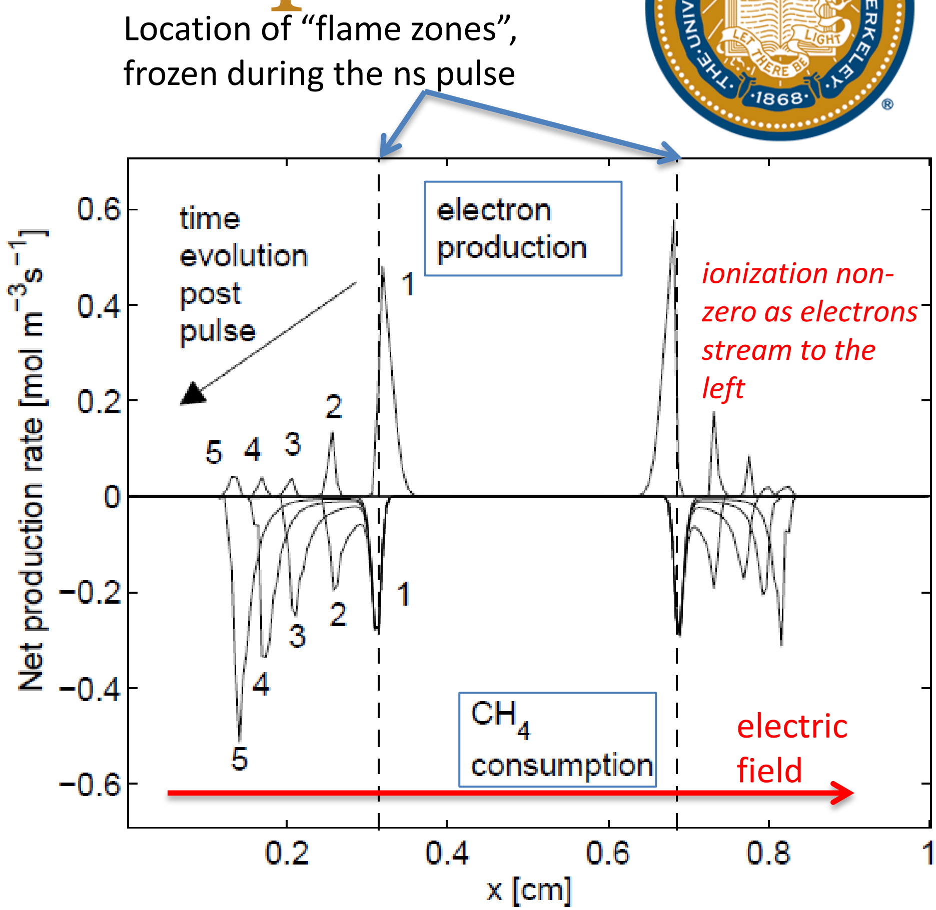

Production rate of electrons (top half plane) and consumption of CH4 (bottom half plane) during the pulse at five time instants corresponding to 1, 4, 8, 12, and 16 ns labeled "1" to "5".

Berkeley UNIVERSITY OF CALIFORNIA

Radical production

- Radical populations build up rapidly during the pulse as CH_4 and O_2 are fragmented by electron impact, by factors of 100 to 1000
- OH is not formed during the pulse, but begins to build up post pulse due to radical recombination

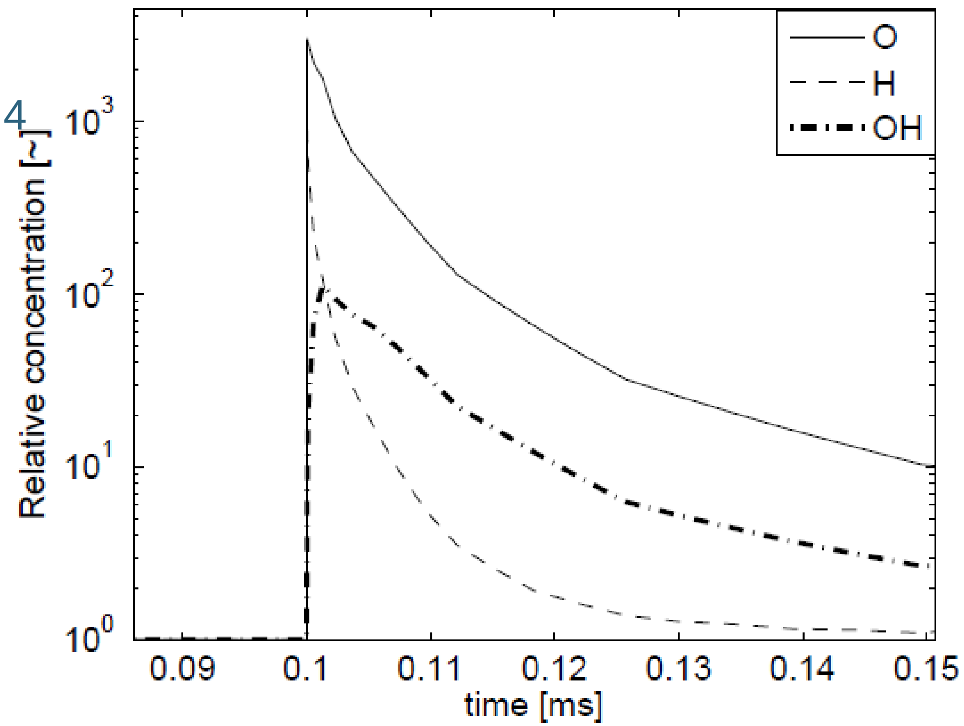

Evolution of domain integrated major radical species concentrations for a 35 ns pulse normalized by the evolution in the unsupported case

Berkeley
UNIVERSITY OF CALIFORNIA

Effect of pulse length

- Longer pulse widths increase radical populations. 25% decrease in pulse width (35ns to 26ns) reduces population by factor of 5

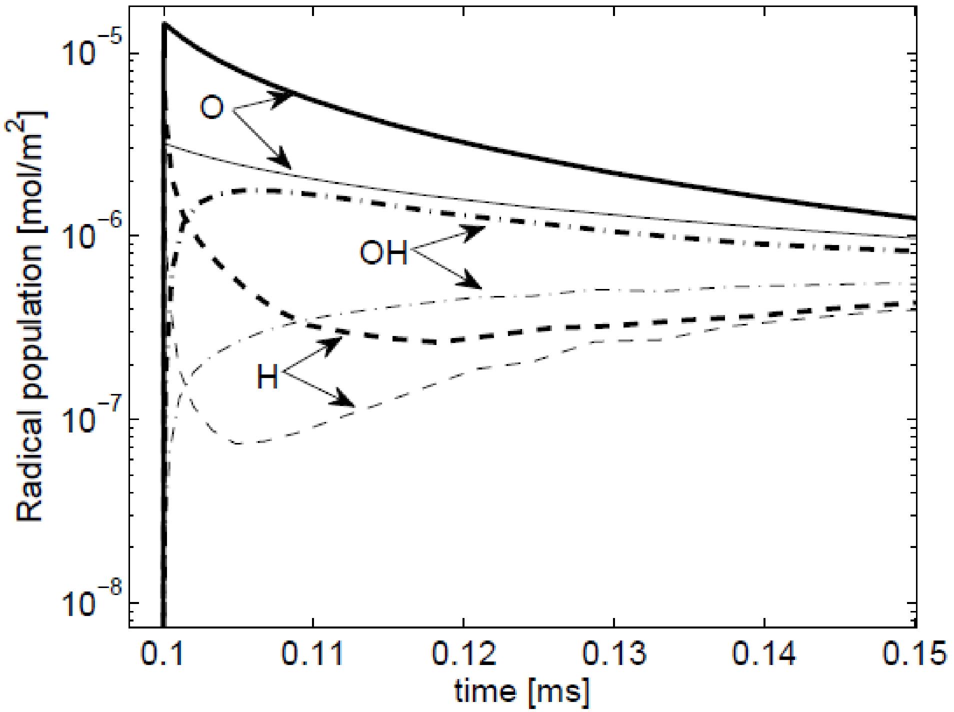

Evolution of total populations of major radical species for a 35 ns (solid lines) and 26 ns (dashed lines) pulse.

Berkeley
UNIVERSITY OF CALIFORNIA

Fresh gas radicals

Fresh gas radical spatial profiles (near left electrode), profiles are separated in time by 4 ns during the pulse, with the post pulse profiles taken at 1 ns, 56 ns, 1.7 µs, and 8.2 µs after the pulse has ended.

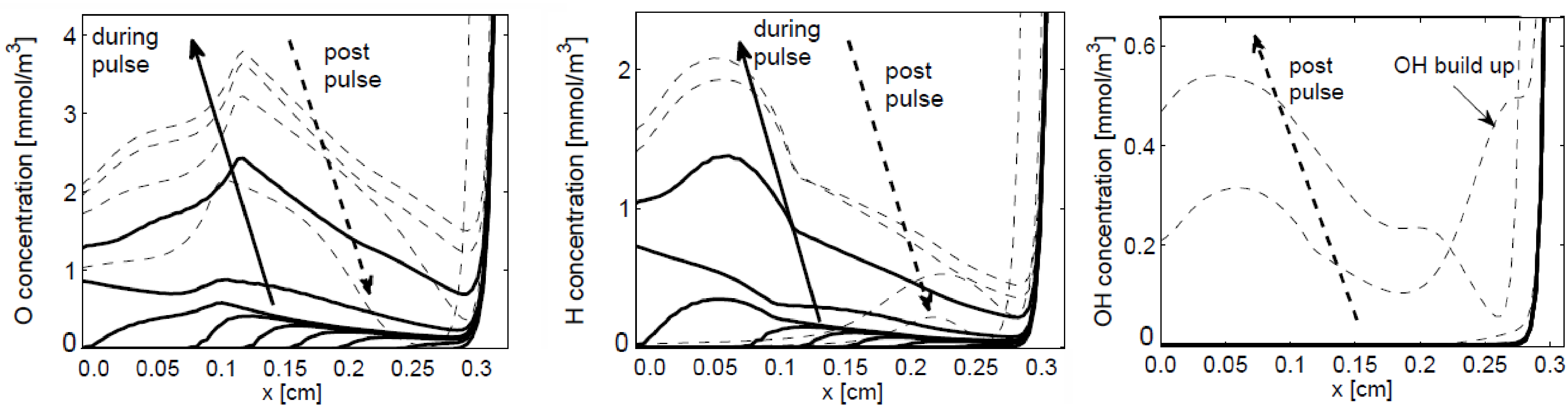

- populations slowly build up (solid lines) before reaching maxima in the vicinity of the boundary electrode (at electron temperature peak)
- OH build up post pulse in the vicinity of the flame zones

Heat release rate

- Post-pulse, the heat-release rate decays rapidly but begins to plateau as the OH build up reaches its maximum
- This sustained heat release accelerates the flames forward into the fresh gases
- After a few ms the enhancement effect dissipates

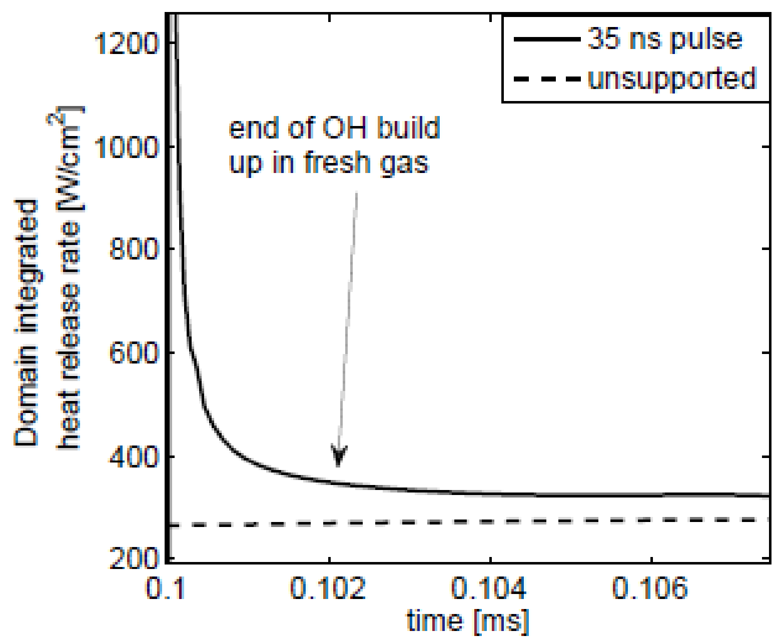

domain integrated heat release rate in the post-pulse period for a 35 ns pulse (solid line) and the unsupported case (dashed line).

Results: global effect on ignition enhancement

flame kernel "size" – separation of heat release fronts

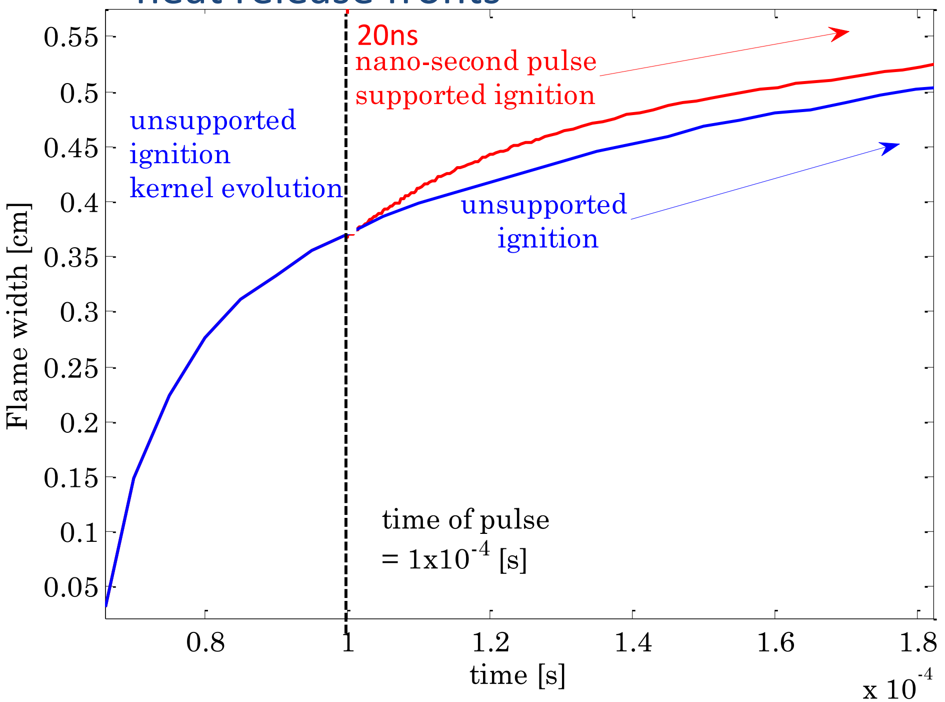

Mass of fuel burned

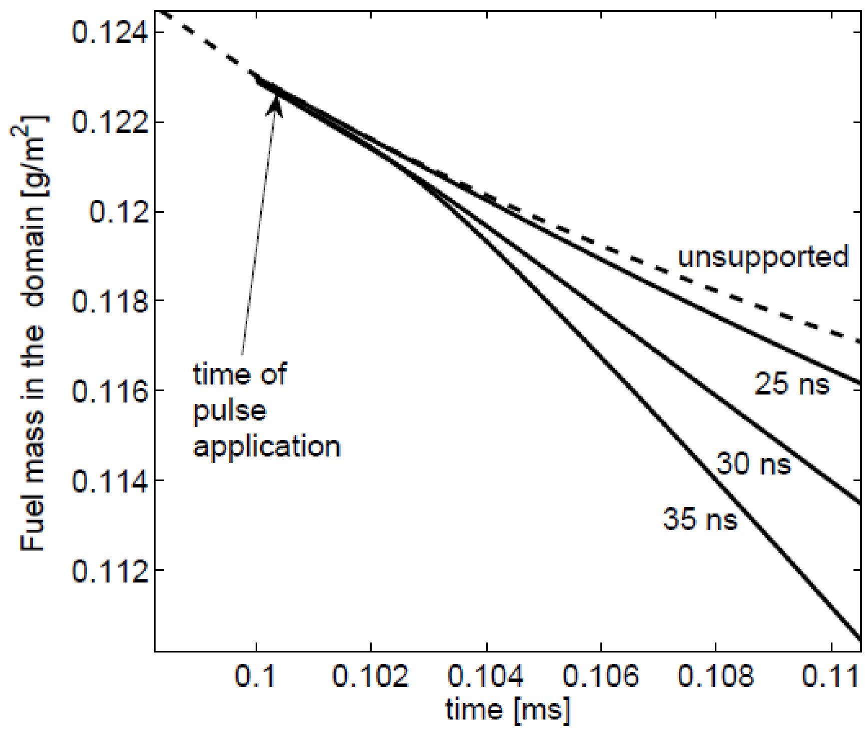

- Supported ignition kernel grows spatially and consumes fuel more rapidly

Berkeley
UNIVERSITY OF CALIFORNIA

Summary

- At equivalent times, up 4% increase in flame kernel size, 6% increase in mass of fuel burned as a result of DC pulse
- With respect to kernel development time, up 12% reduction in time to achieve equivalent flame kernel sizes, 33% reduction in time to achieve equivalent fuel burn
- At longer times, enhancement effect appears to diminish as the supporting effect of burned gas thermal diffusion on the flames decreases (competing effects)
- electron processes in the hot burned-gases are essentially insignificant, due to low electric field and deactivation of energetic electrons by collisions with H_2O

Thanks!

Questions?

Berkeley
UNIVERSITY OF CALIFORNIA